



OPEN

SUBJECT AREAS:

METAL-ORGANIC
FRAMEWORKS

SYNTHESIS AND PROCESSING

Received
2 December 2013Accepted
22 April 2014Published
13 May 2014Correspondence and
requests for materials
should be addressed to
Q.M.G. (qmgao@
buaa.edu.cn)

Constructing Free Standing Metal Organic Framework MIL-53 Membrane Based on Anodized Aluminum Oxide Precursor

Yunlu Zhang¹, Qiuming Gao¹, Zhi Lin³, Tao Zhang⁴, Jiandong Xu¹, Yanli Tan¹, Weiqian Tian¹ & Lei Jiang^{1,2}

¹Key Laboratory of Bio-inspired Smart Interfacial Science and Technology of Ministry of Education, Beijing Key Laboratory of Bio-inspired Energy Materials and Devices, School of Chemistry and Environment, Beihang University, Beijing 100191, P. R. China, ²Institute of Chemistry, Chinese Academy of Sciences, Beijing 100190, P. R. China, ³State Key Laboratory for Advanced Metal Materials, University of Science and Technology of Beijing, Beijing 100083, P. R. China, ⁴Beijing Centre for Physical & Chemical Analysis, Beijing 100089, P. R. China.

Metal organic framework (MOF) materials have attracted great attention due to their well-ordered and controllable pores possessing of prominent potentials for gas molecule sorption and separation performances. Organizing the MOF crystals to a continuous membrane with a certain scale will better exhibit their prominent potentials. Reports in recent years concentrate on well grown MOF membranes on specific substrates. Free standing MOF membranes could have more important applications since they are independent from the substrates. However, the method to prepare such a membrane has been a great challenge because good mechanical properties and stabilities are highly required. Here, we demonstrate a novel and facile technique for preparing the free standing membrane with a size as large as centimeter scale. The substrate we use proved itself not only a good skeleton but also an excellent precursor to fulfill the reaction. This kind of membrane owns a strong mechanical strength, based on the fact that it is much thinner than the composite membranes grown on substrates and it could exhibit good property of gas separation.

Metal organic framework (MOF) materials possessing of well-ordered and controllable pores have become a hot spot in scientific research, because this kind of materials have a great potential performance in gas molecule separation, storage, catalysis, sensor, proton conductivity and so forth¹⁻⁴. Although MOF crystals share a similarity in either structure-regular pores or properties with zeolites, it has been proved challenging to fabricate MOF membranes since it is difficult for the MOF crystals to form strong coordination bonds with the native substrates⁵. Choosing a suitable support or pretreating the substrate is important for forming the dense and continuous MOF membranes. Two categories of supports have usually been used: the nonporous (Au, silicon wafers, graphite and sapphire et al.) and porous (α -Al₂O₃, copper net et al.). Hermes⁶ et al. grew MOF-5 thin films on a gold substrate by introducing a patterned COOH/CF₃-terminated self-assembled monolayer (SAM) on top of the gold substrate aiming at enhancing the covalent attachment. They also prepared a denser coating with intergrown MOF-5 crystals onto the c-plane sapphire substrate deposited with an amorphous Al₂O₃-type buffer layer⁷. Biemmi⁸ et al. reported HKUST-1 membrane grown on differently terminated SAMs on gold substrates. Kitagawa⁹ et al. reported MOF nanofilm on a solid NAFS-1 substrate. There are also some reports on the growth of MOF membranes on porous substrates, among which α -Al₂O₃ is a preferential candidate. For example, Arnold¹⁰ et al. achieved [Mn(HCO₂)₂] on α -Al₂O₃; Yoo¹¹ et al. reported MOF-5 membrane on α -Al₂O₃; Gascon¹² et al. obtained HKUST-1 on α -Al₂O₃. Guo¹³ et al. adopted pre-oxidized copper net to deposit HKUST-1. Besides, organic polymers¹⁴ have also been developed for the deposition or blending of MOFs. The preparation method is also the key to get the MOF membranes with high quality. The generally useful method to prepare MOF membranes is the in situ growth with pre-seeding method or secondary growth. In Ranjan's report¹⁵, the seeds were deposited by manually rubbing the crystals onto PEI coated α -Al₂O₃, and this was a physically attached seeds. Different kinds of chemical seeds have also invented. Yoo et al. used a microwave-induced thermal deposition. His group also demonstrated a thermal deposition pre-seeding method¹⁶, in which

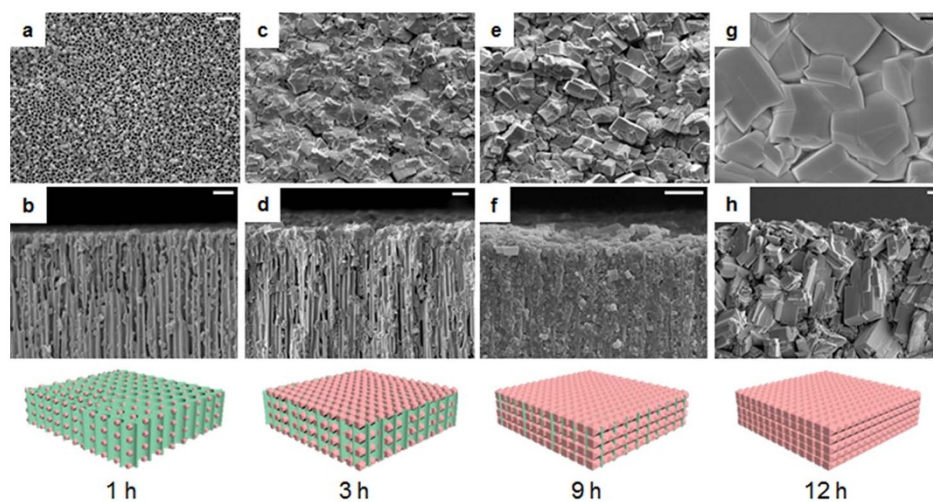


Figure 1 | The simulation models and the SEM images of four characteristic states of the membrane representing the reaction process. The upper line is surface and lower line is the corresponding cross section. (a, b) 1 h in the autoclave, small seed crystals grew on the surface and in the channels and the basic morphology of the AAO membrane remained; 3 h later (c, d), more crystals grew forming a thin layer about one or two hundred nanometer's thick, while the AAO pores were barely seen; 9 h longer in the oven (e, f), crystals grew bigger and the channels got very crowded; and 12 h finally, a free standing MIL-53 membrane was obtained (g, h). The related simulation models are listed accordingly below for clarity. Scale bar, 1 μm .

HKUST-1 crystals in a synthesis solution was dropping onto hot (200°C) $\alpha\text{-Al}_2\text{O}_3$ supports, followed by sonication and in situ growth. McCarthy¹⁷ et al. dropped the organic linker solution, instead, onto the hot substrates and achieved a well-intergrown ZIF-8 membrane. Kitagawa¹⁸ et al. gave a 'Modular assembly' strategy to prepare Cu TCPP nanofilm on quartz substrate. Nan¹⁹ et al. gave a so called step-by-step seeding procedure, in which the substrate was immersed, in sequence, into the organic linker solution and metal ion solution one by one for several cycles. His group has also invented a reactive seeding method²⁰. The $\alpha\text{-Al}_2\text{O}_3$ substrate acts not only as a support, but also as the aluminum precursor. A MOF seed layer formed on the surface in the first in situ growth process when only organic linker was added there. Those approaches were used to enhance the quality of MOF membranes on the substrates. However, inevitably, the morphologies of these membranes are more or less influenced by the substrates, and the applications were strictly limited by the substrates. So, free standing membranes are highly urgent.

Recently, there were several reports on preparation of the free standing MOF membranes. Qiu²¹ et al. used a modified PMMA-PMAA layer on Si substrate to grow the HKUST-1 crystals and obtained the free standing membrane by resolving the organic layer. Li²² et al. used HKUST-1 crystal doped electrospun fibrous materials as skeletons to fabricate the membrane, after second growth a continuous membrane was obtained, in which the crystals doped in the fibrous worked as seed. Both the procedures were complicated and the membranes quality need optimize. Very recently, Zhu²³ et al. demonstrated a free standing MOF-5 membrane using a liquid-liquid interfacial coordination method. However, the membranes were quite fragile and cannot be available in large scale. Peng²⁴ et al. claimed a way to synthesize a free-standing HKUST-1 membrane from copper hydroxide nanostrands at room temperature for gas separation.

In this paper, we develop a novel technique to prepare a free standing MOF MIL-53²⁵ membrane in centimeter scale by choosing anodized aluminum oxide (AAO) disc^{26–28} as the reacting aluminum precursor to cooperate with the organic linker (1,4-benzenedicarboxylic (H_2BDC)) under the facile hydrothermal condition. This method is superior compared with those mentioned above. There is no need to pretreat the substrate or any excessive procedures to obtain a free standing MOF membrane. Besides, this kind of

membrane owns a strong mechanical strength, which as far as we have searched, no articles have ever reported before, even though it is much thinner (about 60 μm in thickness) than the normal $\alpha\text{-Al}_2\text{O}_3$ supported MOF composite membrane showing its amazing application potentials.

Results

Preparation and characterization. In order to get the MIL-53 membrane with no cracks, the AAO disc fabricated based on the electrochemical technique from complete and well crystallized Al metal disc (purity $\geq 99.9\%$) were chosen as the precursor. Figure 1 shows the SEM results of the surfaces and channels of the time dependent reaction process, together with the corresponding schematic diagrams. This reaction was occurred in the autoclave containing AAO disc, H_2BDC and H_2O . At beginning, after 1 h in the autoclave, only a few MIL-53 small crystals appeared on the surface and channels of AAO (Fig. 1a and 1b). Figure 1a is the image of the surface of the membrane. Many small MIL-53 crystals distributed randomly on the bounding sites of the pores and most of the AAO pores are exposed. There are also a lot of small MIL-53 crystals growing on the walls of the channels based on the observation of the SEM on the cross section view (Fig. 1b). The crystals have grown along the channels (see Fig S1), demonstrating that the whole part of the AAO is active with the H_2BDC molecules. 3 h later (Fig. 1c), more and more MIL-53 crystals are in sight, the AAO pores are barely seen, and only from the few defects can we see the pristine pores. From the cross section view (Fig. 1d), we can see that a thin layer about one or two hundred nanometer's thick was formed, and there are some bigger MIL-53 crystals in the channels, some of which were able to stuff the tubes. However, most channels remain what they were and the thickness of the tube wall shows no obvious decrease. 9 h later in the oven (Fig. 1e and 1f), big crystals in rhomb shape are full of sight and some even grow to one micrometer. Great amount of MIL-53 crystals have continuously grown in the channels, making the channels a very crowded place. What is noteworthy is that the tube walls of the AAO channels have been corroded badly, many of which have disappeared. Though some still exist, they are quite not what they were. 12 h later finally, a totally different membrane appeared (Fig. 1g and 1h) with no original sign of AAO disc and only big MIL-53 crystals intergrow with each other in all directions. The SEM images of the central parts of the channels

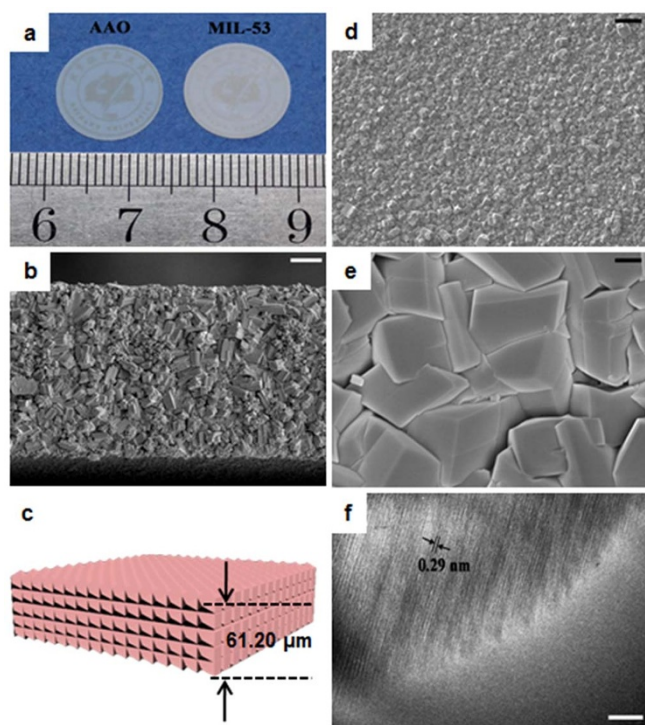


Figure 2 | The digital picture and SEM images the free standing MIL-53 membrane. (a), digital camera photo tells us the difference between AAO and MIL-53 membranes: the latter is much whiter and less transparent than the former. (b), the cross section SEM image of the whole membrane, telling the total vision of the free standing membrane. (c) the simulation model of the membrane with a thickness of 61.20 μm . (d), the image enlarged 1000 times shows the morphology of the crystals and reveals the homogeneity of this membrane in large scale and no defects or cracks can be found. (e), the image further enlarged, crystals intergrow well with each other. And (f), HRTEM image of this membrane demonstrating that the membrane is well crystallized. Scale bar, 10 μm (in (b)), 1 μm (in (d, e)) and 3 nm (in (f)).

after different reaction time are shown in Figure S1. Here, reaction time is definitely responsible for the changing morphology of these series of membranes.

Figure 2a shows the macroscopic image of the prepared MIL-53 membrane. Compared with the pristine AAO membrane, it was whiter and less transparent. But the area is definitely equal to the AAO's, with a diameter of 13 mm. Figure 2b is the cross section SEM

image of the free standing MIL-53 membrane, no pristine AAO channels could be observed and only MIL-53 big crystals intergrow with each other. The total thickness of the membrane is about 60 μm with the simulation model given in Figure 2c, which is similar to that of the AAO. Figure 2d is the SEM image of the membrane magnified at a factor of 1000, no cracks or defects could be found on the surface and the membrane is perfect completely in the whole sight. Even enlarged only 350 times (Figure S2), the membrane is continuous and complete. Further magnifying (Fig. 2e), big grains are everywhere with mostly in similar size and most of them are single crystals. From the HRTEM image (Fig. 2f) of the MIL-53 membrane, we can further see that the crystals were well crystallized with the d-spacing of 0.29 nm in consistent with the (304) lattice plane.

X-ray diffractions were used to determine the structure of the prepared MIL-53 membranes. Figure 3a shows the XRD patterns of the prepared MIL-53 membrane and the simulated pattern referred from the article²⁵. The main 2θ peaks at 8.9° , 10.4° , 12.7° , 15.4° and 17.8° match well with that of MIL-53 from the Cambridge Crystallographic Data Center (No. CCDC-220475). This result indicates that the MIL-53 membrane has a homogeneously phase with the same crystalline structure as that of the MIL-53 powders. Because the MIL-53 crystals may show different diffraction patterns under different preparing conditions²⁵, e.g. as synthesis MIL-53 with BDC occupying the pores, high temperature treated MIL-53 with empty pores and low temperature MIL-53 with H_2O occupying the pores. The XRD patterns of our membrane are in consistent with that of the as synthesis MIL-53 with BDC occupying the pores. A broad background could be observed, indicating that there may be some amorphous Al_2O_3 (unreacted AAO) in the membrane. No preferential orientation of the MIL-53 could be observed for the membrane. The patterns of the respective membranes prepared after different reaction times showed the changes in intensity of the main MIL-53 peaks (see Fig. S3). The patterns of needle-like powder collected at the bottom of the autoclave after reaction show the exactly same patterns as the one of H_2BDC (see Fig. S4), indicating that the powder at the bottom was the unreacted organic linker and no extra MIL-53 crystal peaks exist in the powder collected. This result indicates that the whole MIL-53 crystals are growing on the disc and there are no lose at all.

Thermogravimetry (TG) experiments were performed to take a look at the composition of this membrane (Fig. S5). There are mainly two weight drops between room temperature and 700°C in the TG curves. The first weight drop from 100 to 500°C with a total loss of 19.32 wt.% is due to the departure of the free disordered BDC in the pores of MIL-53. The second weight drop (observed 50.91 wt.%) is due to the elimination of BDC linkers from the framework when the

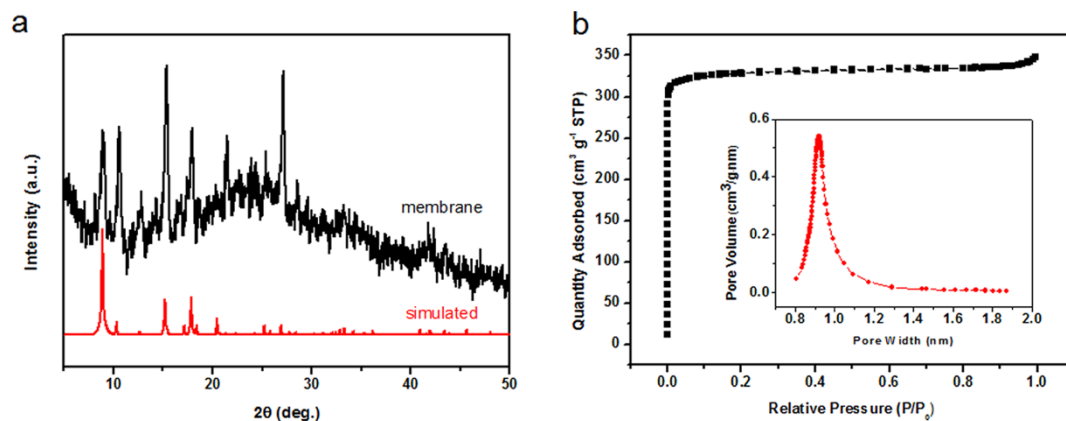


Figure 3 | XRD patterns and BET tests (a). XRD patterns of the free standing MIL-53 membrane and the simulated MIL-53 powders. Characteristic peaks indicate the right crystallization of MIL-53. (b), N_2 sorption isotherms of free standing MIL-53 membrane. Typical I curves are observed, indicating uniform microporous structure. The inset is pore size distribution, showing the main pore size 0.9 nm.

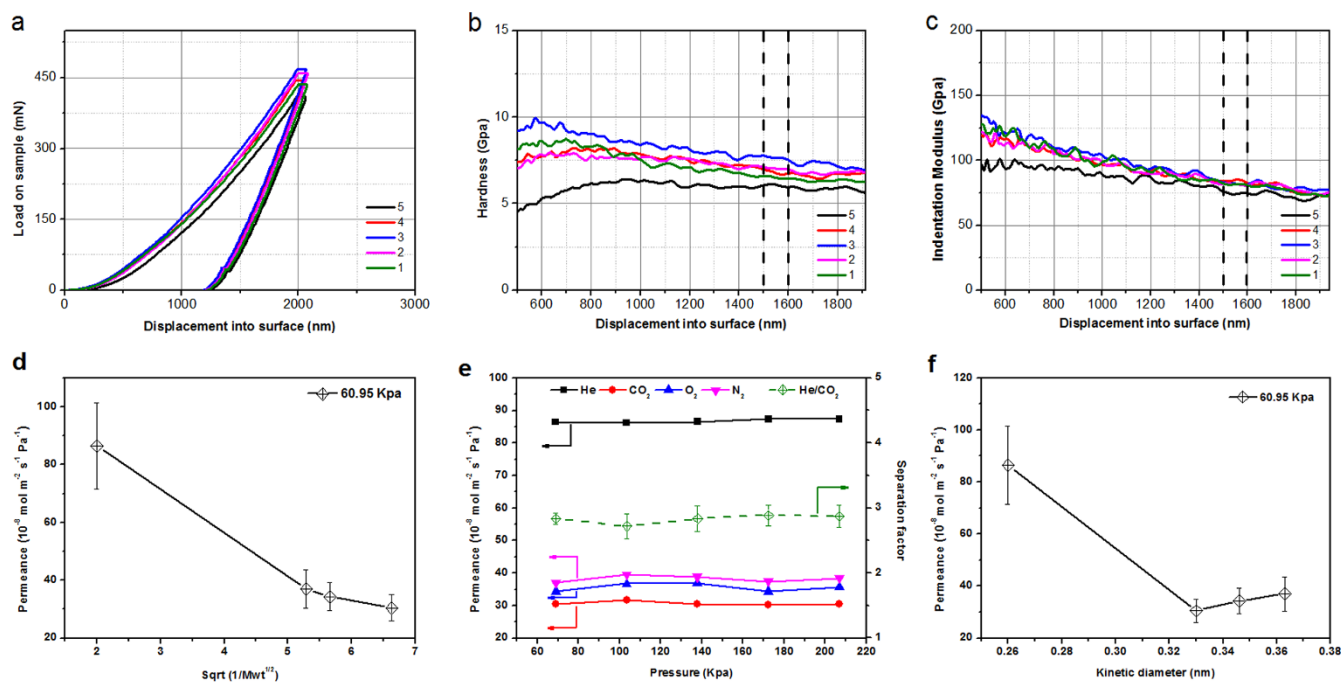


Figure 4 | Mechanical properties and single gas permeance. (a). Typical force-displacement as measured by nano-indentation. (b). the hardness and (c), indentation modulus reached a mean value of 7.01 ± 0.6 Gpa, 82.4 ± 0.7 Gpa (the black line was omitted because of a relative big error). (d), single gas permeance as a function of the inversion of the square root of molecule weight showed a liner relationship which attributed to Knudson diffusion. (e), single gas permeance as a function of transmembrane pressure drop showed almost stable horizontal lines as the pressure increases, indicating that the main transport mechanism of simple gases through the membrane could be Knudson diffusion. The separation factor of the membrane for He/CO₂ was relatively stable as the pressure increases. And (f), single gas permeance as a function of kinetic diameter gave a clear conclusion that this membrane showed ability of less permeance for CO₂ and O₂.

temperature is between 500 and 600 °C. Above 600 °C, the MIL-53 crystals are transformed into amorphous Al₂O₃. The total weight of Al₂O₃ is about 29.77 wt.%, which could include two kinds of sources: one is derived from the MIL-53 phase transformation and the other is resulting from the unreacted AAO. In view of those consideration and calculation, the composition of the as prepared membrane could be as following: MIL-53 crystals (85.6 wt.%) and unreacted Al₂O₃ from AAO substrate (14.4 wt.%), where the MIL-53 crystals is made up of (Al(OH)(O₂C-C₆H₄-CO₂)·(O₂C-C₆H₄-CO₂)_{0.4}).

Energy dispersive spectrum (EDS, given in Fig. S6) has also been used to analyze the composition of the as prepared MIL-53 membrane. Both the surface and cross section of the membrane have been tested. According to the weight percentages of each element given by the EDS test results and using the MIL-53 crystal composition (Al(OH)(O₂C-C₆H₄-CO₂)·(O₂C-C₆H₄-CO₂)_{0.4}) from the TG measurement, we could obtain that the composition of this membrane is MIL-53 88.2 wt.% and unreacted AAO 11.8 wt.% for the surface and MIL-53 87.4 wt.% and AAO 12.6 wt.% for the cross section, which are close to the TG results.

These analyses are in consistent with the XRD patterns which show a broad background. Thus, the MIL-53 membranes we prepared are composed of mainly MIL-53 crystals with a certain amount of unreacted AAO (Al₂O₃). However, the rest AAO (Al₂O₃, 12 ~ 14 wt.%) is not enough to support the whole membrane, and the membrane could be taken as a free standing membrane.

The infrared (IR) spectra of the membrane are in good agreement with that of the MIL-53²⁵ (see Fig. S7). The vibrational bands in the usual region of 1400–1700 cm⁻¹ refer to the carboxylic function. The absorption bands located at 1604 and 1503 cm⁻¹ are assigned to -CO₂ asymmetric stretching, whereas the bands at 1435 and 1414 cm⁻¹ are assigned to -CO₂ symmetric stretching. These values are consistent with the presence of CO₂⁻ groups that are coordinated

to aluminum. The vibrational bands in the region 3600–3500 cm⁻¹ correspond to the stretching modes of water.

N₂ adsorption-desorption analyses results of the prepared MIL-53 membrane were given in Figure 3b. Clearly type-I adsorption and desorption curves could be observed with the mean equivalent pore diameter of 0.9 nm and the BET surface area of 1180 m² g⁻¹. The pore size is well consistence with the MIL-53 structure. No meso- or macropores could be found for the membrane indicating the formation of MIL-53 membrane with no cracks.

Mechanical and gas separation properties. Due to the fact that most MOF materials are synthesized in the typical solvothermal conditions and the products are always powders with micrometer-sized crystallites, limits do exist in the experimental verification of the mechanical properties of these materials. The first reported IRMOF-1 mechanical properties using nanoindentation on a micrometer-sized crystallite with the tip of an atomic force microscopy (AFM) yielded a Young's modulus of 2.7 Gpa, about one in ten of the predicted theoretically for this MOF type. Bundschuh²⁹ firstly reported the mechanical property of HKUST-1 films with a relative higher Young's modulus of 10 Gpa, substantially stiffer than normal polymers (Young's moduli in the range of 0.2 to 5 Gpa). Ortiz³⁰, this year, reported the mechanical properties of MIL-53 (Al) crystals using first principles calculations and showed that the Young's modulus of this soft material could range from 0.9 to 94.7 Gpa because of the existence of anisotropy. Here, we report the mechanical properties of the prepared free standing MIL-53 membrane using standard indentation method which could repeat measurements several times on the same membrane. It is commonly assumed that for indentation depths of less than 10% of total film thickness, the measured values correspond to the real film properties. In this case, the depth we choose to analyze is within 2 μm, which is only 1/30 of the total thickness of the membrane (60 μm). As Figure 4a, 4b, and 4c



illustrates, the mean values of both the hardness and the indentation modulus are 7.01 ± 0.6 Gpa, 82.4 ± 0.7 Gpa (values between 1500 ~ 1600 nm). According to Ortiz's theoretical value by calculation, the Young's modulus value for this material is very anisotropic, with high-value lobes in y direction (60.9 Gpa) as well as along two directions in the xz plane (94.7 Gpa). Our value is in very good agreement with it. This property may be related to the crystal-like structure of the MOF material. The possible explanation for the stiffness of this MIL-53 membrane is that elastic deformation requires to some extent stretching of the ionic (Al^{3+} -carboxylate) bonds and covalent (C-C single and double) bonds in the MOF.

These free standing membranes were then used to investigate the separation performance of gases. Figure 4d, 4e, and 4f are the permeance of gas molecules (He , CO_2 , O_2 , and N_2) at room temperature as function of their molecular weights, pressure drops and kinetic diameters, respectively. Figure 4d shows a liner relationship between the permeance and the square root of the inversion of the gas molecular weights. This indicates that the permeation behaviors mainly follow the Knudson diffusion law. It is reasonable for the Knudson type transport of small gas molecules through MIL-53 membrane because the size of MIL-53 pores (0.9 nm) is relatively bigger than the kinetic diameters of the gas molecules (He : 0.26 nm, CO_2 : 0.33 nm, O_2 : 0.35 nm, and N_2 : 0.36 nm). Figure 4e gives that the single gas permeances of each gas on these membranes show almost stable horizontal lines as the pressure increases. This result further indicates that the main transport mechanism of simple gases through the membrane could be Knudson diffusion. The separation factor of the membrane for He/CO_2 is about 2.9 and is relatively stable under different pressure drops. Apparently, the permeation values of He are much higher than those three gases, for example, at a pressure of 60.95 Kpa (Fig. 4f), the permeances ($10^{-8} \text{ mol m}^{-2} \text{ s}^{-1} \text{ Pa}^{-1}$) for each gas are: He 88.4, CO_2 30.5, O_2 34.3, and N_2 37.0, with a selective factors (He/CO_2 , He/O_2 , and He/N_2) of 2.9, 2.6, and 2.4, respectively. This membrane shows a property of less permeance for CO_2 , mainly because there is a strong adsorption between CO_2 molecules and MIL-53 crystals pore walls. This cooperation behavior could serve as the driving force to separate CO_2 from gas mixtures. Besides, this membrane also shows an affinity with O_2 . We consider that maybe this effect has relationship with the delocalization π bond in 1,4-benzenedicarboxylic and the strong electronegativity of O_2 molecular. Few articles reported this before and more concentrated on the CO_2 when it is related to gas permeation³¹⁻³⁴. Pressure at 30 psi, more than 2 times of the standard atmospheric pressure, has been tested on the thin membranes, showing the stable mechanical advantage, which is consistent with the mechanical tests results.

Discussion

In summary, we prepared a free standing MIL-53 membrane by sacrificing AAO membrane to cooperate with H_2BDC under mild hydrothermal condition. Controlling the reaction time, membranes with different corrosion status were achieved. A free standing MIL-53 membrane has been formed after 12 h with a size as large as centimeter scale and the thickness of the membrane equivalent with that of AAO. These membranes we prepared are composed of mainly MIL-53 crystals (86 ~ 88 wt.%) with the rest unreacted AAO (12 ~ 14 wt.%). They also shows good mechanism strength which the hardness and modulus reached as high as 7.01 ± 0.6 Gpa, 82.4 ± 0.7 Gpa. Besides, this membrane shows a specific property for gas separation. The CO_2 permeance is the smallest followed by other three different gases as O_2 , N_2 and He .

Methods

Materials preparation. Our experiments were based on this simple reaction: $\text{AAO} + \text{H}_2\text{BDC} \rightarrow \text{MIL-53}$. All the reactants are used without further purification. The process was as following. First, a rounded disc (0.014 g) with 13 mm of diameter and 60 μm of thickness after washing with deionized water was horizontally placed at the bottom of the Teflon liner autoclave (23 mL), and then H_2BDC (0.144 g) together

with pure water (10 g) was added in the autoclave. And after sealing, the whole object was putted in a process controlling oven to reach a demanding temperature (140°C) with a speed of 1°C per minute for different but specific periods. Second, allowed to cool to room temperature, pure water was used to wash the product and 100°C oven was maintained 10 h to dry those membranes. Finally, the membranes with different corrosion conditions were obtained.

Characterization. The crystalline phases of MIL-53 membranes were determined using X-ray diffractometry (Labx XRD-6000, Shimadzu, Japan) with $\text{Cu K}\alpha$ radiation (wavelengths $\lambda = 0.15418$ nm) in the range of $5^\circ \leq 2\theta \leq 50^\circ$ (scan speed $5^\circ/\text{min}$ and scan step 0.02°) at room temperature. SEM images of the membrane were observed via scanning electron microscopy (SEM) (Quanta-250 FEG, Holland) with 5 kV voltage and 10 μA current and a working distance 8 ~ 10 mm. A thin layer of gold was coated on the specimens to increase its conductivity. TG experiments were performed in air with a heating rate $10^\circ\text{C}/\text{min}$ using a TGA Q500 instrument. For the TEM measurement of the MIL-53 membranes, a small piece of membrane was glued on the Mo metal circle with $\Phi = 3$ mm, and then the specimens were thinned by conventional mechanical polishing and the Ar-iron milling with 4.2 keV at 5° glancing incidence by Gantan model 691 precision ion polishing system for 4 h until a pore appeared in the eyepiece. Observations were made at 200 kV on a JEOL JEM-2100F microscope with field-emission gun. Nitrogen isotherm at 77 K was obtained using a surface area and pore size analyzer (Micromeritics ASAP 2020) for 6 pieces of the prepared membrane. The sample was degassed at 330°C for 12 h. The mechanical strength tests were taken on the nanoindenter (Agilent XP, USA). Infrared (IR) spectra of the membrane were obtained by the spectrophotometer (Nicolet iN10 MX, USA). Energy dispersive X-ray spectrum (EDS) was obtained on the Field-emission Scanning electron microscopy (7500F).

Gas permeation tests. Gas permeation experiments were performed on single gas equipment at room temperature. The membrane was firstly pasted on a PET ring with an outer and inner diameter 25 mm and 10 mm using an epoxy resin and cured at room temperature for more than 12 h. Then the membrane was placed in an O-ring sealed module. The membrane permeance was then determined as a function of time for which a soap film rose 20 cm distance.

- Li, H., Eddaoudi, M., O'Keeffe, M. & Yaghi, O. M. Design and synthesis of an exceptionally stable and highly porous metal-organic framework. *Nature* **42**, 276–279 (1999).
- Li, J. R., Kuppler, R. J. & Zhou, H. C. Selective gas adsorption and separation in metal-organic frameworks. *Chem. Soc. Rev.* **38**, 1477–1504 (2009).
- Dybtsev, D. N., Chun, H., Yoon, S. H., Kim, D. & Kim, K. Microporous manganese formate: a simple metal-organic porous material with high framework stability and highly selective gas sorption properties. *J. Am. Chem. Soc.* **126**, 32–33 (2004).
- Xu, G., Otsubo, K., Yamada, T., Sakaida, S. & Kitagawa, H. Superprotonic conductivity in a highly oriented crystalline metal-organic framework nanofilm. *J. Am. Chem. Soc.* **135**, 7438–7441 (2013).
- Shah, M., McCarthy, M. C., Sachdeva, S., Lee, A. K. & Jeong, H. K. Current status of metal-organic framework membranes for gas separations: promises and challenges. *Ind. Eng. Chem. Res.* **51**, 2179–2199 (2011).
- Hermes, S., Schröder, F., Chelmoski, R., Wöll, Christof. & Fischer, R. A. Selective nucleation and growth of metal-organic open framework thin films on patterned COOH/CF₃-terminated self-assembled monolayers on Au(111). *J. Am. Chem. Soc.* **127**, 13744–13745 (2005).
- Hermes, S., Zacher, D., Baunemann, A., Wöll, C. & Fischer, R. A. Selective growth and MOCVD loading of small single crystals of MOF-5 at alumina and silica surfaces modified with organic self-assembled monolayer. *Chem. Mater.* **19**, 2168–2173 (2007).
- Biemmi, E., Scherb, C. & Bein, T. Oriented growth of the metal organic framework $\text{Cu}_3(\text{BTC})_2(\text{H}_2\text{O})_3 \cdot x\text{H}_2\text{O}$ tunable with functionalized self-assembled monolayers. *J. Am. Chem. Soc.* **129**, 8054–8055 (2007).
- Makiura, R. et al. Surface nano-architecture of a metal-organic framework. *Nat. Mater.* **9**, 565–571 (2010).
- Arnold, M. et al. Oriented crystallization on supports and anisotropic mass transport of the metal-organic framework manganese format. *Eur. J. Inorg. Chem.* **1**, 60–64 (2007).
- Yoo, Y., Lai, Z. & Jeong, H. K. Fabrication of MOF-5 membranes using microwave-induced rapid seeding and solvothermal secondary growth. *Micropro. Mesopro. Mat.* **123**, 100–106 (2009).
- Gascon, J., Aguado, S. & Kapteijn, F. Manufacture of dense coatings of $\text{Cu}_3(\text{BTC})_2$ (HKUST-1) on α -alumina. *Micropro. Mesopro. Mat.* **113**, 132–138 (2008).
- Guo, H., Zhu, G., Hewitt, I. J. & Qiu, S. "Twin copper source" growth of metal-organic framework membrane: $\text{Cu}_3(\text{BTC})_2$ with high permeability and selectivity for recycling H_2 . *J. Am. Chem. Soc.* **131**, 1646–1647 (2009).
- Ren, H., Jin, J., Hu, J. & Liu, H. Affinity between metal-organic frameworks and polyimides in asymmetric mixed matrix membranes for gas separations. *Ind. Eng. Chem. Res.* **51**, 10156–10164 (2012).
- Ranjan, R. & Tsapatsis, M. Microporous metal organic framework membrane on porous support using the seeded growth method. *Chem. Mater.* **21**, 4920–4924 (2009).



16. Guerrero, V. V., Yoo, Y., McCarthy, M. C. & Jeong, H. K. HKUST-1 membranes on porous supports using secondary growth. *J. Mater. Chem.* **20**, 3938–3943 (2010).
17. McCarthy, M. C., Guerrero, V. V., Barnett, G. & Jeong, H. K. Synthesis of zeolitic imidazolate framework films and membranes with controlled microstructure. *Langmuir* **26**, 14636–14641 (2010).
18. Xu, G., Yamada, T., Otsubo, K., Sakaida, S. & Kitagawa, H. Facile “Modular assembly” for fast construction of a highly oriented crystalline MOF nanofilm. *J. Am. Chem. Soc.* **134**, 16524–16527 (2012).
19. Nan, J., Dong, X., Wang, W., Jin, W. & Xu, N. Step-by-step seeding procedure for preparing HKUST-1 membrane on porous α -alumina support. *Langmuir* **27**, 4309–4312 (2011).
20. Hu, Y. *et al.* Metal-organic framework membranes fabricated via reactive seeding. *Chem. Commun.* **47**, 737–739 (2011).
21. Ben, T., Lu, C., Pei, C., Xu, S. & Qiu, S. Polymer-supported and free-standing metal-organic framework membrane. *Chem. Eur. J.* **18**, 10250–10253 (2012).
22. Wu, Y., Hannamb, P. & Li, G. Electrospun fibrous mats as skeletons to produce free-standing MOF membranes. *J. Mater. Chem.* **22**, 16971–16978 (2012).
23. Lu, H. & Zhu, S. Interfacial synthesis of free-standing metal-organic framework membranes. *Eur. J. Inorg. Chem.* **8**, 1294–1300 (2013).
24. Mao, Y. *et al.* Room temperature synthesis of free-standing HKUST-1 membranes from copper hydroxide nanostrands for gas separation. *Chem. Commun.* **49**, 5666–5668 (2013).
25. Loiseau, T. *et al.* A rationale for the large breathing of the porous aluminum terephthalate (MIL-53) upon hydration. *Chem. Eur. J.* **10**, 1373–1382 (2004).
26. Woo, L., Ran, J., Ulrich, G. & Kornelius, N. Fast fabrication of long-range ordered porous alumina membranes by hard anodization. *Nat. Mater.* **5**, 741–747 (2006).
27. Yoo, Y. & Jeong, H. K. Rapid fabrication of metal organic framework thin films using microwave-induced thermal deposition. *Chem. Commun.* 2441–2443 (2008).
28. Maksoud, M., Roques, N., Brandès, S., Arurault, L. & Sutter, J. P. Efficient growth of sub-micrometric MOF crystals inside the channels of AAO membranes. *J. Mater. Chem. A* **1**, 3688–3693 (2013).
29. Bundschuh, S. *et al.* Mechanical properties of metal-organic framework: An indentation study on epitaxial thin films. *Appl. Phys. Lett.* **101**, 101910-1 ~ 4 (2012).
30. Ortiz, A. U., Boutin, A., Fuchs, A. H. & Coudert, F. X. Metal-organic frameworks with wine-rack motif: what determines their flexibility and elastic properties? *J. Chem. Phys.* **138**, 174703-1 ~ 8 (2013).
31. Bux, H. *et al.* Zeolitic imidazolate framework membrane with molecular sieving properties by microwave-assisted solvothermal synthesis. *J. Am. Chem. Soc.* **131**, 16000–16001 (2009).
32. Zhao, Z., Ma, X., Li, Z. & Lin, Y. S. Synthesis, characterization and gas transport properties of MOF-5 membranes. *J. Mem. Sci.* **382**, 82–90 (2011).
33. Perez, E. V., Balkus, Jr. K. J., Ferraris, P. J. & Musselman, I. H. Mixed-matrix membranes containing MOF-5 for gas separations. *J. Mem. Sci.* **328**, 165–173 (2009).
34. Pan, Y. & Lai, Z. Sharp separation of C2/C3 hydrocarbon mixtures by zeolitic imidazolate framework-8 (ZIF-8) membranes synthesized in aqueous solutions. *Chem. Commun.* **47**, 10275–10277 (2011).

Acknowledgments

Financial supports by National Basic Research Programs of China (973 Programs, No. 2011CB935700 and 2014CB931800), Chinese Aeronautic Project (No. 2013ZF51069) and Chinese National Science Foundation (No. U0734002) are gratefully acknowledged.

Author contributions

Q.-M.G. planned and supervised the project; L.J. and Q.-M.G. advised on the project; Y.-L.Z. and Q.-M.G. designed and performed experiments; Z.L. carried out the mechanical property tests; T.Z. performed the BET tests; Q.-M.G., Y.-L.Z., J.-D.X., Y.-L.T. and W.-Q.T. analyzed data; Q.-M.G. and Y.-L.Z. wrote the manuscript; and all authors discussed the results and commented on the manuscript.

Additional information

Supplementary information accompanies this paper at <http://www.nature.com/scientificreports>

Competing financial interests: The authors declare no competing financial interests.

How to cite this article: Zhang, Y.L. *et al.* Constructing Free Standing Metal Organic Framework MIL-53 Membrane Based on Anodized Aluminum Oxide Precursor. *Sci. Rep.* **4**, 4947; DOI:10.1038/srep04947 (2014).



This work is licensed under a Creative Commons Attribution-NonCommercial-NoDerivs 3.0 Unported License. The images in this article are included in the article's Creative Commons license, unless indicated otherwise in the image credit; if the image is not included under the Creative Commons license, users will need to obtain permission from the license holder in order to reproduce the image. To view a copy of this license, visit <http://creativecommons.org/licenses/by-nc-nd/3.0/>